

# Crystal Structure of an Archaeal Pentameric Riboflavin Synthase in Complex with a Substrate Analog Inhibitor

## STEREOCHEMICAL IMPLICATIONS\*

Received for publication, August 26, 2005, and in revised form, October 26, 2005 Published, JBC Papers in Press, November 4, 2005, DOI 10.1074/jbc.M509440200

Arne Ramsperger<sup>†,2</sup>, Martin Augustin<sup>†,3</sup>, Ann-Kathrin Schott<sup>§4</sup>, Stefan Gerhardt<sup>‡4</sup>, Tobias Krojer<sup>‡5</sup>, Wolfgang Eisenreich<sup>§</sup>, Boris Illarionov<sup>§</sup>, Mark Cushman<sup>¶</sup>, Adelbert Bacher<sup>§</sup>, Robert Huber<sup>‡</sup>, and Markus Fischer<sup>§6</sup>

From the <sup>†</sup>Max-Planck-Institut für Biochemie, Abteilung für Strukturforschung, Am Klopferspitz 18, D-82152 Martinsried, Germany,

the <sup>§</sup>Lehrstuhl für Organische Chemie und Biochemie, Technische Universität München, Lichtenbergstrasse 4, D-85747 Garching, Germany, and the <sup>¶</sup>Department of Medicinal Chemistry and Pharmacology, Purdue University, West Lafayette, Indiana 47907

Whereas eubacterial and eukaryotic riboflavin synthases form homotrimers, archaeal riboflavin synthases from *Methanocaldococcus jannaschii* and *Methanothermobacter thermoautrophicus* are homopentamers with sequence similarity to the 6,7-dimethyl-8-ribityllumazine synthase catalyzing the penultimate step in riboflavin biosynthesis. Recently it could be shown that the complex dismutation reaction catalyzed by the pentameric *M. jannaschii* riboflavin synthase generates riboflavin with the same regiochemistry as observed for trimeric riboflavin synthases. Here we present crystal structures of the pentameric riboflavin synthase from *M. jannaschii* and its complex with the substrate analog inhibitor, 6,7-dioxo-8-ribityllumazine. The complex structure shows five active sites located between adjacent monomers of the pentamer. Each active site can accommodate two substrate analog molecules in anti-parallel orientation. The topology of the two bound ligands at the active site is well in line with the known stereochemistry of a pentacyclic adduct of 6,7-dimethyl-8-ribityllumazine that has been shown to serve as a kinetically competent intermediate. The pentacyclic intermediates of trimeric and pentameric riboflavin synthases are diastereomers.

Riboflavin (vitamin B<sub>2</sub>) serves as the precursor of flavin mononucleotide (FMN) and flavin adenine dinucleotide (FAD), essential cofactors for several oxidoreductases that are indispensable in most living cells. The work on riboflavin biosynthesis in microorganisms has been covered extensively in recent reviews (1–4). Riboflavin is biosynthesized in plants, many bacteria, and in fungi but not in animals. Therefore, enzymes of this pathway have been proposed to be attractive targets for antimicrobial strategies (5–7).

\* This work was supported by National Institutes of Health Grant UO1 CA89566 as well as by support from grants from the Deutsche Forschungsgemeinschaft, the Fonds der Chemischen Industrie, and the Hans-Fischer-Gesellschaft. The costs of publication of this article were defrayed in part by the payment of page charges. This article must therefore be hereby marked "advertisement" in accordance with 18 U.S.C. Section 1734 solely to indicate this fact.

The atomic coordinates and structure factors (code 2B98 (native enzyme) and 2B99 (DORL complex)) have been deposited in the Protein Data Bank, Research Collaboratory for Structural Bioinformatics, Rutgers University, New Brunswick, NJ (<http://www.rcsb.org/>).

<sup>†</sup> These authors have contributed equally to this work.

<sup>‡</sup> To whom correspondence may be addressed. Tel.: 49-89-8578-2678; Fax: 49-89-8578-3516; E-mail: ramsperg@biochem.mpg.de.

<sup>§</sup> Present address: Proteros Biostuctures GmbH, Am Klopferspitz 19, D-82152 Martinsried, Germany.

<sup>¶</sup> Present address: AstraZeneca, Protein Structure Laboratory, 26F14 Mereside, Alderley Park, Macclesfield SK104TG, England.

<sup>5</sup> Present address: Inst. für Molekulare Pathologie (IMP), Dr. Bohrgasse 7, A-1030 Wien, Austria.

<sup>6</sup> To whom correspondence may be addressed. Tel.: 49-89-289-13336; Fax: 49-89-289-13363; E-mail: markus.fischer@ch.tum.de.

In the final steps of the biosynthetic pathway, lumazine synthase (LS) catalyzes the condensation of the pyrimidinedione (1) with 3,4-dihydroxy-2-butane-4-phosphate (2) to release water, inorganic phosphate and 6,7-dimethyl-8-ribityllumazine (DMRL)<sup>7</sup> (8, 9), and riboflavin synthase (RS) catalyzes a dismutation of DMRL (3) affording riboflavin (4) and 5-amino-6-ribitylamino-2,4(1H,3H)-pyrimidinedione (1) (Fig. 1); more specifically, that reaction involves the transfer of a four-carbon moiety between two DMRL molecules serving as donor and acceptor, respectively (10–13). Both reactions are thermodynamically irreversible (9, 14) and can proceed in the absence of a catalyst (11, 15–17).

LS from fungi are  $c_5$ -symmetric homopentamers, whereas the enzymes from plants, Archaea, and most eubacteria studied are 532 symmetric capsids of 60 identical subunits, which are best described as dodecamers of pentamers. The subunit folding patterns of pentameric and icosahedral LS are similar. In *Bacillaceae*, lumazine synthase and riboflavin synthase form a complex comprising an icosahedral capsid of 60 lumazine synthase subunits and a core of three riboflavin synthase subunits; historically, these unusual enzyme complexes were designated heavy riboflavin synthase (18, 19). Riboflavin synthases from eubacteria are homotrimers where each subunit folds into two topologically similar domains, but the protein fails to obey trigonal symmetry. An active site is formed at the interface between the C-terminal domain of one subunit (serving as the donor site with regard to transfer of a four-carbon moiety) and the N-terminal domain of an adjacent subunit (serving as acceptor site) (20).

Riboflavin synthases of Archaea show sequence similarity with lumazine synthases. In line with the sequence characteristics, RS from *Methanocaldococcus jannaschii* (MjaRS) has been shown to be a homopentamer in solution (21). This paper reports the crystal structure of that enzyme.

## MATERIALS AND METHODS

*Protein Preparation, Crystallization, and Data Processing*—Cloning, expression, and purification of the protein have been described elsewhere (21). Crystals of wild-type MjaRS were grown at 18 °C using the sitting drop vapor diffusion method by mixing equal amounts of protein (6 mg/ml) in 100 mM potassium phosphate, pH 7.0, containing 30 mM Tris and 2 mM dithiothreitol with a reservoir solution containing 0.1 M HEPES, pH 7.0, and 40% 2-methyl-2,4-pentanediol. Crystals appeared within several days and belonged to space group P1 with cell parameters

<sup>7</sup> The abbreviations used are: DMRL, 6,7-dimethyl-8-ribityllumazine; SeMet, selenomethionine; Mja, *M. jannaschii*; RS, riboflavin synthase; LS, lumazine synthase; MjaRS, RS from *M. jannaschii*; SpoLS, lumazine synthase from *S. pombe*; DORL, 6,7-dioxo-8-ribityllumazine; r.m.s.d., root mean square deviation.

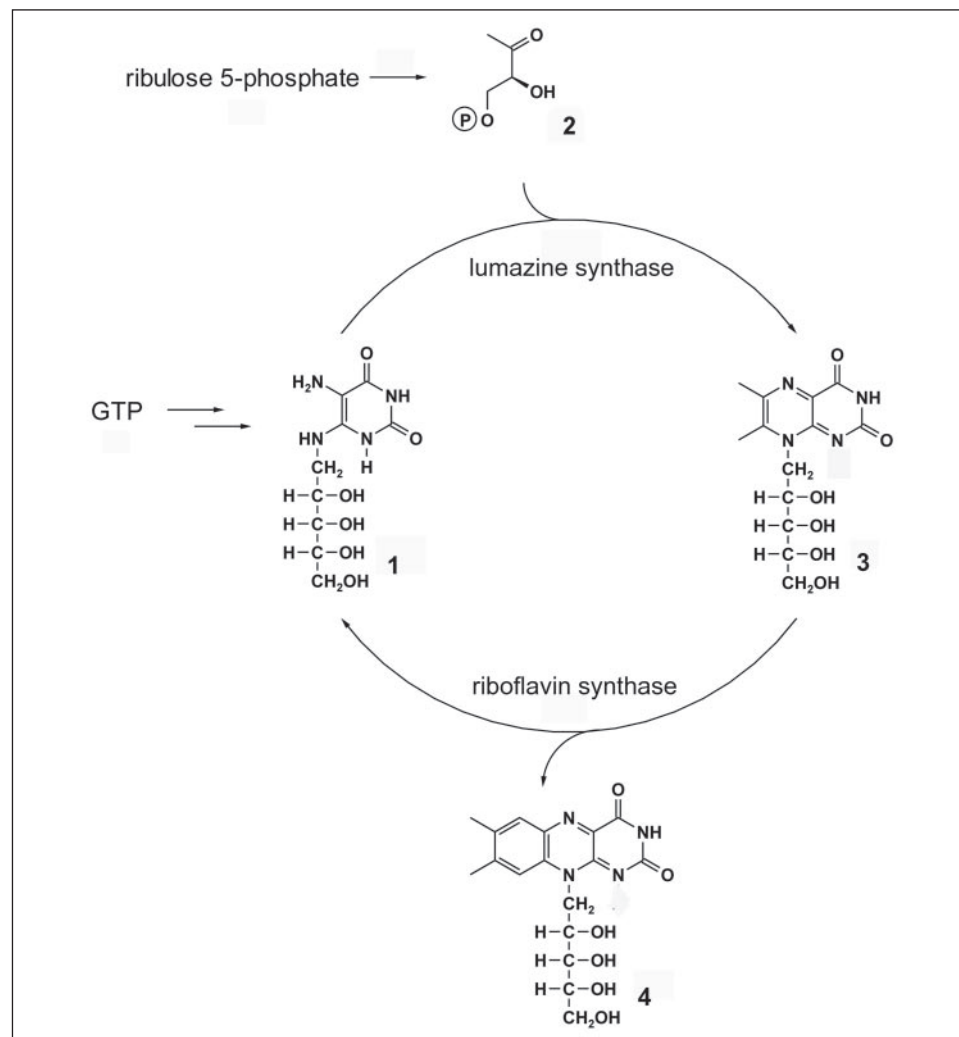


**FIGURE 1. Terminal reactions of the pathway of riboflavin biosynthesis.** 1, 5-amino-6-ribitylaminopyrimidine; 2, 3,4-dihydroxy-2-butanone 4-phosphate; 3, 6,7-dimethyl-8-ribityllumazine; 4, riboflavin.

$a = 41.9 \text{ \AA}$ ,  $b = 72.9 \text{ \AA}$ ,  $c = 72.7 \text{ \AA}$ , and  $\alpha = 68.9^\circ$ ,  $\beta = 74.9^\circ$ ,  $\gamma = 75.1^\circ$  corresponding to five monomers per asymmetric unit. Selenomethionine (SeMet)-substituted MjaRS (6 mg/ml) was crystallized by mixing equal amounts of protein (6 mg/ml) at 18 °C with a reservoir solution containing 0.1 M HEPES, pH 7.3, 0.1 M ammonium sulfate, and 20% polyethylene glycol 4000. The composition of cryoprotectant of the SeMet-substituted crystal was: 25% glycerol, 100 mM potassium phosphate, 100 mM HEPES, pH 7.0. These crystals belonged to space group P6<sub>3</sub>, with cell constants  $a = b = 103.8 \text{ \AA}$ ,  $c = 129.4 \text{ \AA}$  and  $\alpha = \beta = 90^\circ$ ,  $\gamma = 120^\circ$ , also containing five monomers per asymmetric unit.

The protein-inhibitor complex of native MjaRS with 6,7-dioxo-8-ribityllumazine (DORL) was obtained by adding the inhibitor in excess to native crystals. After an incubation period of 2 h, the crystals were flash-frozen in mother liquor in the cryostream. All crystals were measured at 100 K.

Data sets of the native protein and the protein-inhibitor complex were collected with a Mar Research image plate on a Rigaku rotation anode. Data were processed with MOSFLM (22) and scaled and merged with the CCP4 package (23). Data collection statistics are summarized in Table 1.

An single-wavelength anomalous dispersion dataset of SeMet crystals was collected at beamline ID14-4 at the European Synchrotron Radiation Facility (Grenoble, France). Data were processed using DENZO and SCALEPACK (24). Ten selenium positions were located using SnB (25). Refinement of heavy atom parameters and phase calcu-

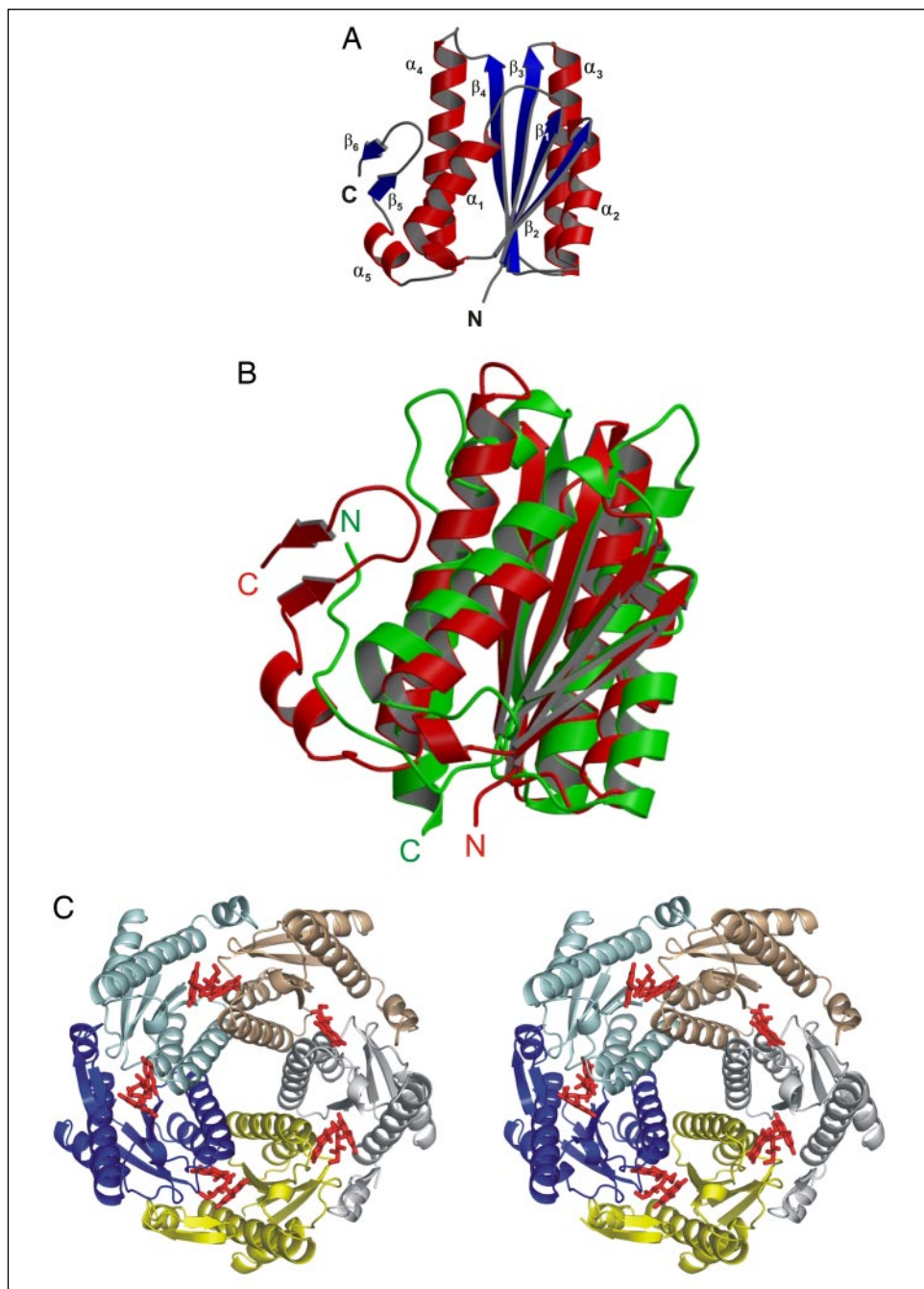
lation was done with SHARP (26). The resulting electron density map was modified and improved by solvent flattening and non-crystallographic averaging in RESOLVE (27). Data collection and phasing statistics are summarized in Table 1.

**Model Building and Refinement**—An initial model of MjaRS (SeMet) was built manually using MAIN (28) and subsequently subjected to several cycles of refinement and manual rebuilding. The structure of native MjaRS was determined by molecular replacement using the program MOLREP of the CCP4 package (23) and the pentamer of the SeMet protein as a search model.

After rebuilding of the model, energy-restrained crystallographic refinement was carried out with maximum likelihood algorithms implemented in CNS (29), using the protein parameters of Engh and Huber (30) or REFMAC (31). Bulk solvent, overall anisotropic  $B$ -factor corrections and non-crystallographic restraints were introduced depending on the behavior of the free  $R$  index. The complex crystals suffered from the soaking procedure and showed a diffraction pattern with large and smeared spots which might explain the rather high  $R$ -values. Nevertheless, the density for the protein and the bound ligands is unambiguous.

**Analysis and Graphical Representation**—The pentacyclic reaction intermediates were energy minimized using SYBYL modeling software (32). Correct atom types, stereocenters, hybridization states, and bond types were defined, and Gasteiger-Hückel charges were assigned to each atom. Positioning of these intermediates in the active site formed

## Structure of Riboflavin Synthase of *M. jannaschii*



between adjacent monomers were carried out using the coordinates of the MjaRS-DORL complex and molecule A as the potential acceptor site. All interactions of molecule A of the complex structure, concerning its pteridine ring system and ribityl side chain persist in the model of the intermediate placed in the active site.

Stereochemical parameters were assessed with PROCHECK (33). Protein structures were three-dimensionally aligned with TOP3D (34), figures were prepared with MOLSCRIPT (35) and PYMOL (36).

**Protein Data Bank Accession Codes**—The coordinates were deposited at the RCSB Protein Data Bank under the accession numbers 2B98 (native enzyme) and 2B99 (DORL complex).

## RESULTS

Recombinant RS of *M. jannaschii* (MjaRS) was expressed and purified as described (21). Crystals of MjaRS grew in space group P1, con-

taining one pentamer in the asymmetric unit. The crystals diffracted to a resolution of 2.3 Å, and the structure was solved by single-wavelength anomalous dispersion using selenomethionine-substituted protein, which was crystallized in the space group P6<sub>3</sub>. An initial model was built in the experimental electron density and was used to position the molecule in the triclinic unit cell. Both crystal forms contain identical pentamers in the asymmetric unit that presumably correspond to the solution state of the protein.

The final model of the pentameric RS of *M. jannaschii* consists of 725 residues with a well defined protein backbone. Poor electron density is present at the C-terminal region for three subunits of the pentamer (residues 143–153), but most of the side chains are clearly defined, except for some surface-exposed residues. The pentamer has a size of roughly 80 × 80 × 45 Å.

The MjaRS-monomer forms a three-layered ( $\alpha\beta\alpha$ ) structure with a

**TABLE 1**

X-ray data processing and final refinement statistics.

Structure	SeMet	Native	Substrate analog complex
<b>Crystal data</b>			
Space group	P6 <sub>3</sub>	P1	P1
Cell constants	$a = b = 103.83 \text{ \AA}$ , $c = 129.43 \text{ \AA}$ $\alpha = 90^\circ$ , $\gamma = 120^\circ$	$a = 41.77 \text{ \AA}$ , $b = 72.69 \text{ \AA}$ , $c = 72.70 \text{ \AA}$ $\alpha = 68.47^\circ$ , $\beta = 74.61^\circ$ , $\gamma = 74.90^\circ$	$a = 41.94 \text{ \AA}$ , $b = 72.91 \text{ \AA}$ , $c = 72.78 \text{ \AA}$ $\alpha = 68.50^\circ$ , $\beta = 74.39^\circ$ , $\gamma = 74.53^\circ$
<b>Data collection</b>			
Wavelength (Å)	0.9793	15,418	15,418
Resolution range (Å) <sup>a</sup>	20.0–3.21	50.0–2.30 (2.38–2.30)	20–2.22 (2.31–2.22)
Completeness (%) <sup>a</sup>	91.7 (93.4) <sup>b</sup>	96.0 (92.2)	90.9 (71.9)
Unique reflections	23,438 <sup>b</sup>	32,165	34,797
Redundancy <sup>a</sup>	2.2 (2.2) <sup>b</sup>	1.9 (1.8)	3.4 (3.2)
$I/\sigma^a$	14.1 (3.5)	12.2 (3.4)	7.9 (2.9)
$R_{\text{sym}}(\%)^a$	4.4 (21.1) <sup>b</sup>	5.0 (24.5)	7.1 (26.0)
<b>Phasing</b>			
Phasing power acentric	0.702		
$R_{\text{cullis}}$	0.899		
Figure of merit			
SHARP	0.220		
RESOLVE	0.485		
<b>Refinement</b>			
Resolution range (Å)		20.0–2.30	20.0–2.22
$R_{\text{cryst}}(\%)$		20.77	25.80
$R_{\text{free}}(\%)^c$		27.56	29.57
r.m.s.d.			
Bonds (Å)		0.010	0.007
Angles (°)		1.233	1.337
<b>Ramachandran plot<sup>d</sup></b>			
Most favored (%)		92.3	93.8
Generously allowed (%)		6.9	5.8
Additionally allowed (%)		0.5	0.3
Disallowed (%)		0.3	0.2
<b>Nonhydrogen protein</b>			
Atoms		5342	5756
Solvent molecules		294	233
<b>Average <math>B</math> values (Å<sup>2</sup>)</b>			
Protein		33.7	29.8
Solvent		44.9	34.2
Inhibitor			37.83

<sup>a</sup> Highest resolution bin in parentheses.<sup>b</sup> Friedel-mates treated as independent reflections.<sup>c</sup>  $R_{\text{free}}$  is the cross-validation  $R$ -factor computed for a test set of 5% of unique reflections.<sup>d</sup> Ramachandran statistics as defined by PROCHECK (33).

parallel four-stranded  $\beta$ -sheet that is flanked on both sides by two  $\alpha$ -helices (Fig. 2A). The secondary structure and topology of the monomer is described as  $\beta_1\alpha_1\beta_2\alpha_2\beta_3\alpha_3\beta_4\alpha_4\alpha_5\beta_5\beta_6$ . The active site is formed by the interface between two subunits of the pentamer. As mentioned above, the partial sequence identity between LS from different organisms and RS of *M. jannaschii* implicates a similar three-dimensional structure. Indeed, both monomer structure and the type and character of the interactions involved in pentamer formation are highly similar to LS. LSs exhibit a three-layered structure ( $\alpha\beta\alpha$ ). The core of the monomer is reminiscent of the flavodoxin fold and consists of a central parallel  $\beta$ -sheet of four strands with topology  $\beta_2\beta_3\beta_4\beta_5$  that is flanked on both sides by the  $\alpha$ -helix motifs  $\alpha_1\alpha_4\alpha_5$  and  $\alpha_2\alpha_3$ , respectively.

A DALI search (37) for similar structures found similarities to numerous proteins with a DMRL fold (SCOP 52121). The top DALI hits are the lumazine synthases from the following organisms: *Brucella abortus* (Protein Data Bank code 1DIO-A, Z-score 18.4, r.m.s.d. for 132 C<sub>α</sub> atoms = 2.2 Å, sequence identity 14%) and *Bacillus subtilis* (Protein Data Bank code 1RVV-1, Z-score 16.7, r.m.s.d. for 129 C<sub>α</sub> atoms = 2.1, sequence identity 22%).

There are also considerable structural similarities to other proteins. One specific example with low sequence identity and an apparently different mode of substrate binding is the D-ribose-binding protein from *Escherichia coli* (Protein Data Bank code 2DRI, Z-score 11.1, r.m.s.d. for 121 C<sub>α</sub> atoms = 2.6 Å, sequence identity 13%).

Despite the small overall deviation between MjaRS and known lumazine synthase structures, there is a significant difference at the C terminus. At this region, MjaRS contains an alpha-helix and a two stranded anti-parallel  $\beta$ -sheet (Fig. 2B). This C-terminal anti-parallel  $\beta$ -sheet of MjaRS is located at the interface between adjacent subunits of the pentamer.

The overall structure of the pentameric assembly of *M. jannaschii* riboflavin synthase viewed along the 5-fold non-crystallographic symmetry axis is shown in Fig. 2C. Details of the refinement and model statistics are given in Table 1.

To identify the active site of the enzyme we soaked crystals of riboflavin synthase with the substrate analog inhibitor DORL. The refinement statistics of the inhibitor complex structure are summarized in Table 1. The overall folding of the enzyme in complex with the inhibitors is identical to that of the native structure (data not shown), except at the C terminus, which is involved in binding of one inhibitor molecule. Consequently this region is better defined by electron density.

The chemical reaction catalyzed by RS requires the binding of two substrate molecules to the catalytically competent active site. In the crystal structure, nine out of these ten positions are occupied by the inhibitor molecules, although with slightly different occupancies as deduced from different temperature factors. The individual subunits of the pentamer are very similar with r.m.s.d. values between 0.1 and 0.36 Å, which is in the range of the experimental error. Pairs of DORL mol-

## Structure of Riboflavin Synthase of *M. jannaschii*

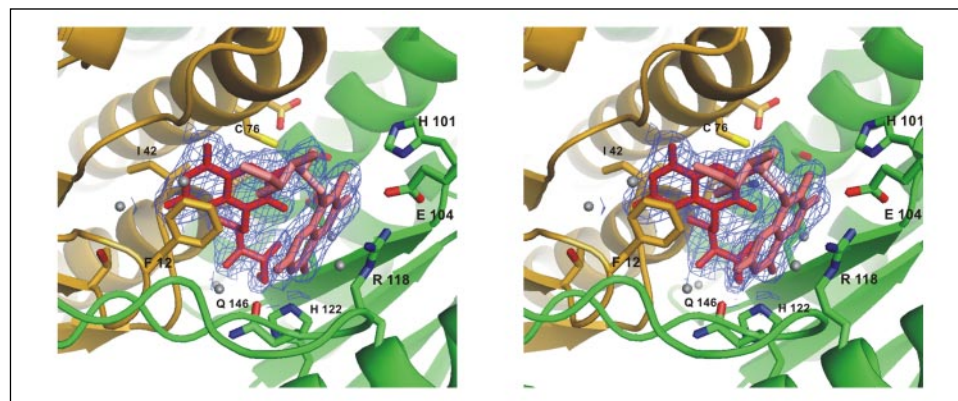
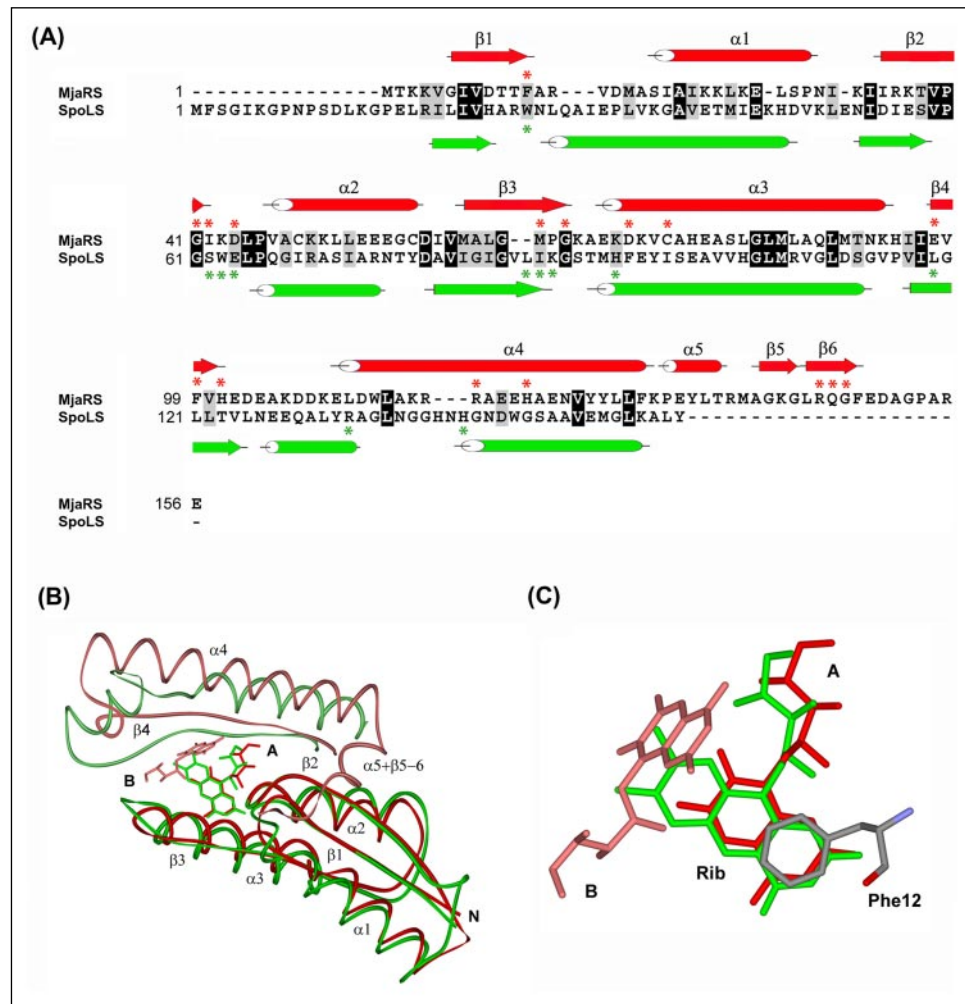


**FIGURE 4.** Stereo view of the final  $2F_0 - F_c$  electron density map, covering the anti-parallel bound substrate analog inhibitors (DORL). The two bound molecules between two adjacent monomers **C** (gold) and **E** (green) are contoured at  $1.0 \sigma$ . Water molecules inside the cavity are shown as gray balls (maximum distance of  $5 \text{ \AA}$  to the inhibitors). The substrate analog inhibitor **A** (red) interacts with monomer **C**, whereas the second inhibitor molecule **B** (pink) shows mainly interactions with monomer **E**.

ecules are located in an anti-parallel orientation in the active site formed by two adjacent subunits facing very different environments (Fig. 3).

The binding of the substrate analog inhibitors shows that one molecule lies at the bottom of the catalytic center and forms a hydrogen bond network with protein subunit C involving its extended ribityl side chain and the pteridine ring-system (Figs. 4 and 5). The ribityl side chain forms hydrogen bonds with the main chain of nitrogen Gly<sup>41</sup>, nitrogen Ile<sup>42</sup>, nitrogen and oxygen Glu<sup>97</sup> and with the  $\gamma$ -carboxyl group of Asp<sup>44</sup> (protein subunit E), and two hydroxyl groups (OH-2, OH-3) are linked to water molecules. In addition, the pteridine ring system of molecule A is sandwiched between the aromatic ring of Phe<sup>12</sup> on one side and Ile<sup>42</sup>

and Cys<sup>76</sup> on the other side (Fig. 5A). The carbonyl O-2 of A is in hydrogen-bonding distance to a water molecule, which in turn makes hydrogen bonds to the side chain of Thr<sup>10</sup> and the backbone carbonyl of Met<sup>66</sup>. The amide group of Ile<sup>42</sup> is directed toward the carbonyl O-2, and a similar interaction is found between the carbonyl O-4 and the backbone amide group of Gly<sup>68</sup> (Fig. 5A).

This rigid fixation of molecule A orients it to the second substrate analog inhibitor (molecule B), bound with anti-parallel orientation at subunit E. The ribityl side chain of molecule B is exposed in the direction of the solvent, and the ribityl hydroxyl groups OH-1 and OH-4 interact with the side chain of Asp<sup>73</sup> (chain C) and a water molecule,

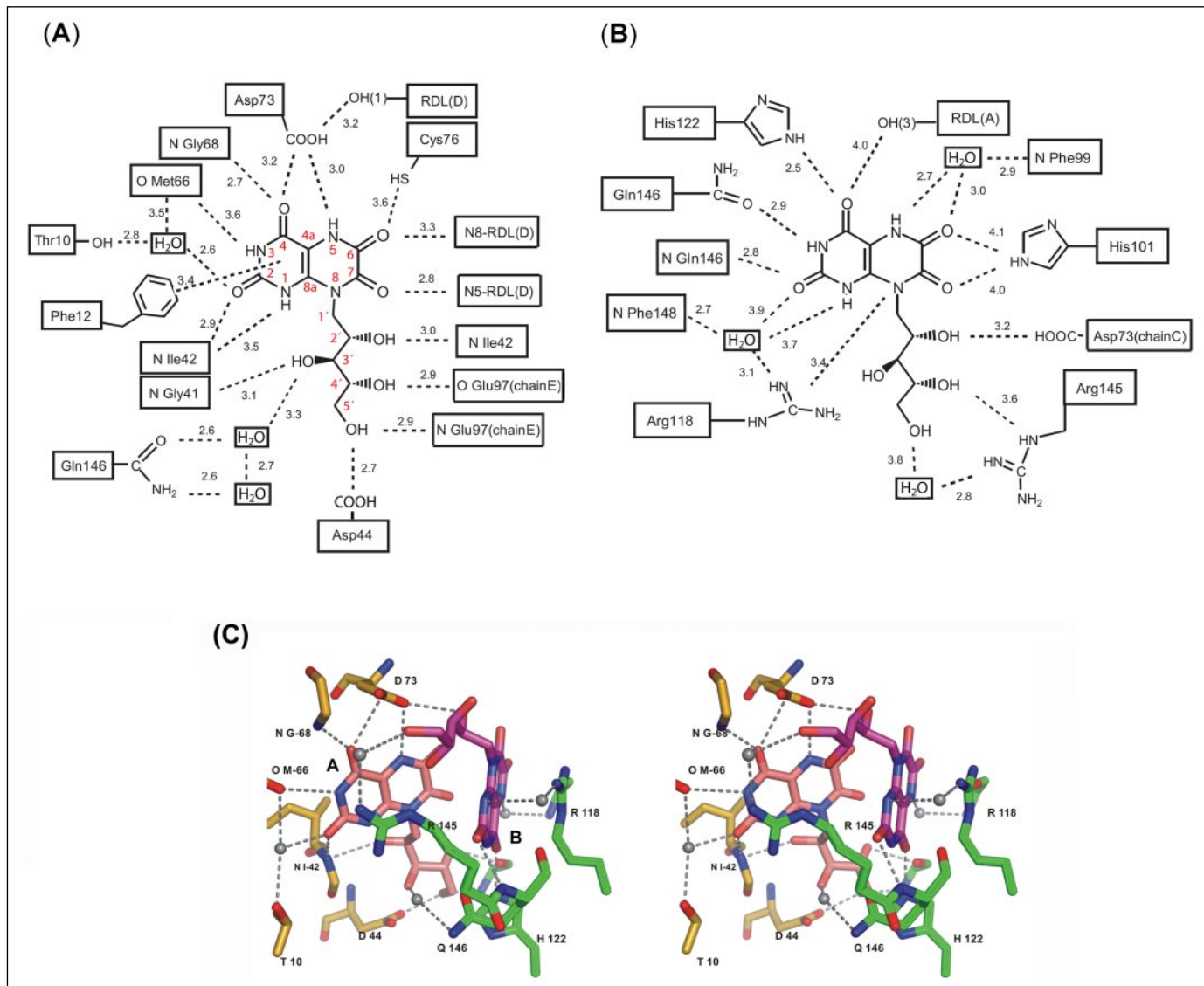


**FIGURE 5.** Bonding topology of 6,7-dioxo-8-ribityllumazine bound to *M. jannaschii* riboflavin synthase. **A**, molecule A (RDL-A) bound at subunit C; **B**, molecule B (RDL-D), with ribityl chain directed to the solvent mainly interacts with subunit E; **C**, three-dimensional presentation of H-bond network involved in substrate binding.

whereas the ribityl hydroxyl group OH-3 is directed to the side chain of Arg<sup>145</sup> (Fig. 5B). The side chain of Arg<sup>118</sup>, which forms a salt-bridge to Glu<sup>104</sup>, lies coplanar to the pteridine ring system. The ε-NH1-group of Arg<sup>118</sup> and O-δ of Glu<sup>104</sup> are in a distance of about 3.5 Å to the N-8. Further hydrogen bonds are observed between the carbonyl O-4 and the side chain of His<sup>122</sup>. The carbonyl O-2 forms a hydrogen bond to the peptide amide group of Gln<sup>146</sup> and to a water molecule, which is coordinated by the backbone groups of O Gln<sup>146</sup>, nitrogen Phe<sup>148</sup>, and N-1 of the pteridine ring-system (Fig. 5, B and C).

Superposition of the four well defined substrate analog inhibitor pairs show no significant differences in the coordination and geometry (data not shown). The two pteridine ring systems are orientated at an angle of ~60°. The pteridine ring system of the natural substrate DMRL has two methyl groups in position 6 and 7, while the inhibitor used in this study has two carbonyl groups at these positions. In the complex structure, the 7-carbonyl-O of molecule A points to the N-5 of molecule B at a distance about 2.8 Å (3.3 Å).

The residues of the active site involved in coordination of the two substrate analog inhibitors are highly conserved in putative archaeal riboflavin synthases (Fig. 6). In all sequences, the phenylalanine stacking

to molecule A is found in a position corresponding to Phe<sup>12</sup> of the MjaRS. Structural superposition of the MjaRS-DORL complex with the *Schizosaccharomyces pombe* LS-riboflavin complex (1KYV (38)) reveals that the pteridine ring system of molecule A lies coplanar to the isoalloxazine ring of riboflavin. Likewise, the ribityl moieties of this substrate analog inhibitor and riboflavin have a similar orientation, suggesting that molecule A marks the acceptor site and molecule B the donor site (Fig. 3).

The residue Ile<sup>42</sup> at the opposite side of the pteridine ring system is also conserved. At position 76 of MjaRS, archaeal riboflavin synthases display a serine or cysteine residue. Similarly for the second binding site (molecule B) of the substrate analog inhibitor, residues Asp<sup>73</sup>, His<sup>101</sup>, Arg<sup>118</sup>, His<sup>122</sup>, and Arg<sup>145</sup> are all invariant in putative archaeal riboflavin synthases (Fig. 6).

## DISCUSSION

Recent studies have identified a pentacyclic intermediate in the reaction trajectories of riboflavin synthases of an eubacterium, *Escherichia coli*, and an Archaeon, *M. jannaschii* which have been designated as Compound Q and Compound Q', respectively (Fig. 7). Whereas these intermediates have identical constitutions, their respective chro-

# Structure of Riboflavin Synthase of *M. jannaschii*

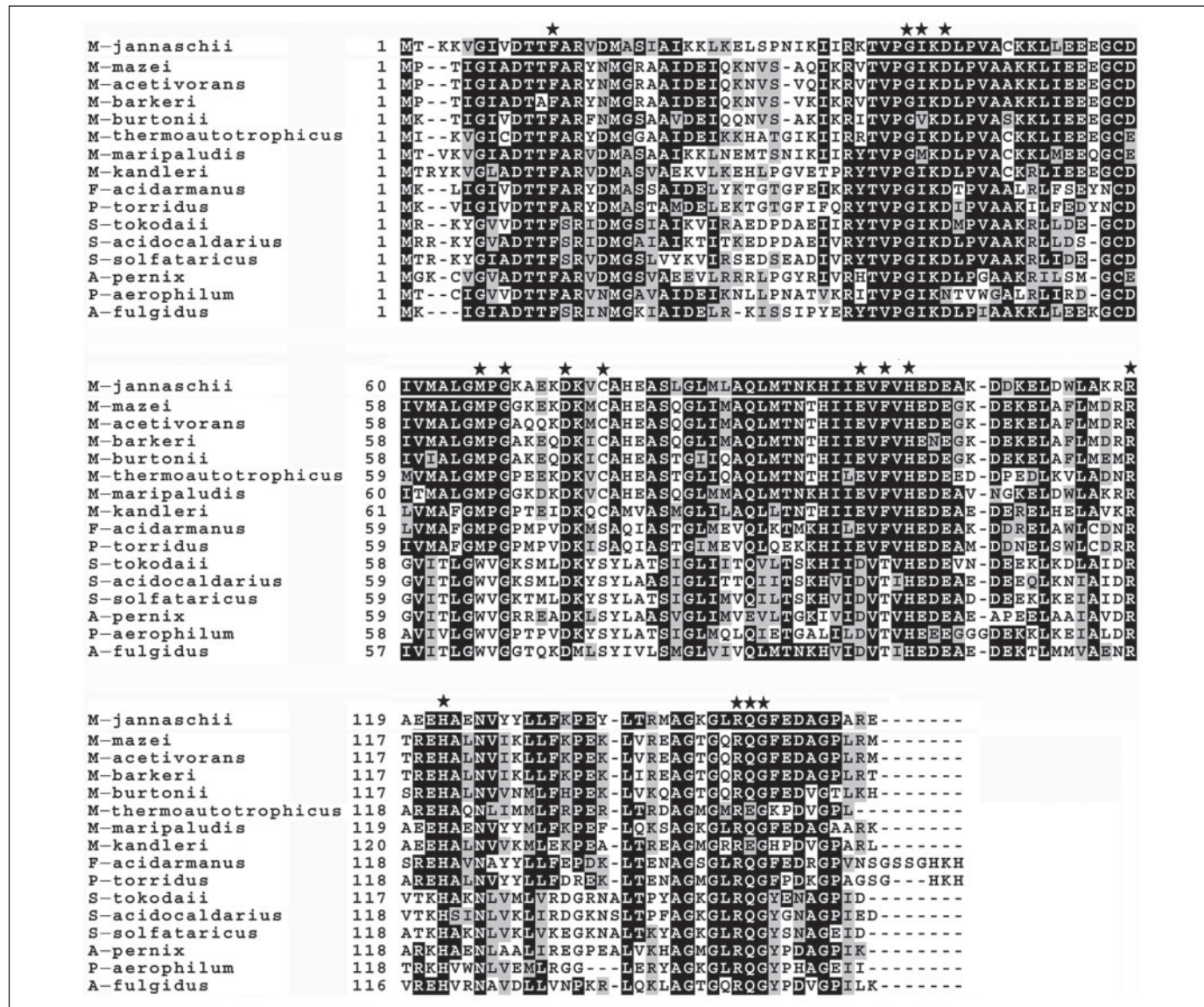


FIGURE 6. Sequence alignment of 16 archaeal type riboflavin synthases. Gaps (denoted as dash) were introduced to optimize alignments. The alignment was produced using the tool CLUSTALW (53) from EMBL-EBI ([www.ebi.ac.uk](http://www.ebi.ac.uk)). Active site residues are marked by asterisks. Strains and GenBank™ accession numbers are as follow: *Aeropyrum pernix* K1 (NP\_147650); *Archaeoglobus fulgidus* DSM 4304 (NP\_070245); *Ferroplasma acidarmanus* (ZP\_00306970); *M. jannaschii* DSM 2661 (NP\_248178); *Methanococcus maripaludis* S2 (NP\_987300); *Methanopyrus kandleri* AV19 (NP\_613646); *Methanoscincus acetivorans* C2A (NP\_61743); *Methanococcoides burtonii* DSM 6242 (ZP\_00148893); *Methanoscincus barkeri* str. *fusaro* (NP\_00296068); *Methanoscincus mazae Goe I* (NP\_632269); *Methanothermobacter thermoautotrophicus str. delta H* (NP\_275277); *Picrophilus torridus* DSM 9790 (YP\_023491); *Pyrobaculum aerophilum str. IM2* (NP\_559706); *Sulfolobus solfataricus* P2 (NP\_341940); *Sulfolobus tokodaii* str. 7 (NP\_376265); *Sulfolobus acidocaldarius* DSM 639 (YP\_255481).

mophores are enantiotopic, and the intermediates *per se* are diastereotopic (since the ribityl side chains invariantly obey D-configuration in both pentacyclic intermediates). Notably, the intermediate Q produced by the eubacterial enzyme can serve as a kinetically competent substrate for the eubacterial but not for the archaeal enzyme; the intermediate Q' produced by the archaeal enzyme is a kinetically competent substrate for the archaeal enzyme and not for the eubacterial enzyme (39).

The absolute stereochemistry of the pentacyclic intermediate of the *E. coli* enzyme could be determined by the comparison between the x-ray structures of the trimeric *E. coli* enzyme (that had been crystallized without a ligand) and an artificial monomeric form of the *S. pombe* enzyme (that had been co-crystallized with 6-carboxyethyl-7-oxo-8-ribityllumazine), and the configurations at the newly formed ring carbons were assigned to be 6*R* and 7*S* (Fig. 7) (20).

The DORL used for soaking experiments in the present study is isospecific with the natural substrate, DMRL. Hence, it appears plausible that

the topological relation of the two inhibitor molecules at the active site emulate the topology of the actual substrate molecules prior to the dismutation reaction. Naturally, that topology defines the sterical constraints for dimer formation. Unless one assumes very far-reaching conformational reorganization at the active site in the course of the reaction (which appears unlikely in light of the rather rigid active site cavity), the only possible stereochemical outcome of the dimerization catalyzed by the pentameric *Mja* riboflavin synthase is the diastereomer Compound Q' with 6*S*/7*R* configuration (Figs. 7 and 8).

We are not aware of any other case in the literature where a given reaction proceeds via diastereomeric intermediates under the catalytic influence of enzymes from two different species. On the other hand, we must assume that the uncatalyzed formation of riboflavin from DMRL is bound to proceed via both possible stereochemical trajectories, although the free energy difference of the two diastereomers should result in different velocities. In any case, the stereochemical information

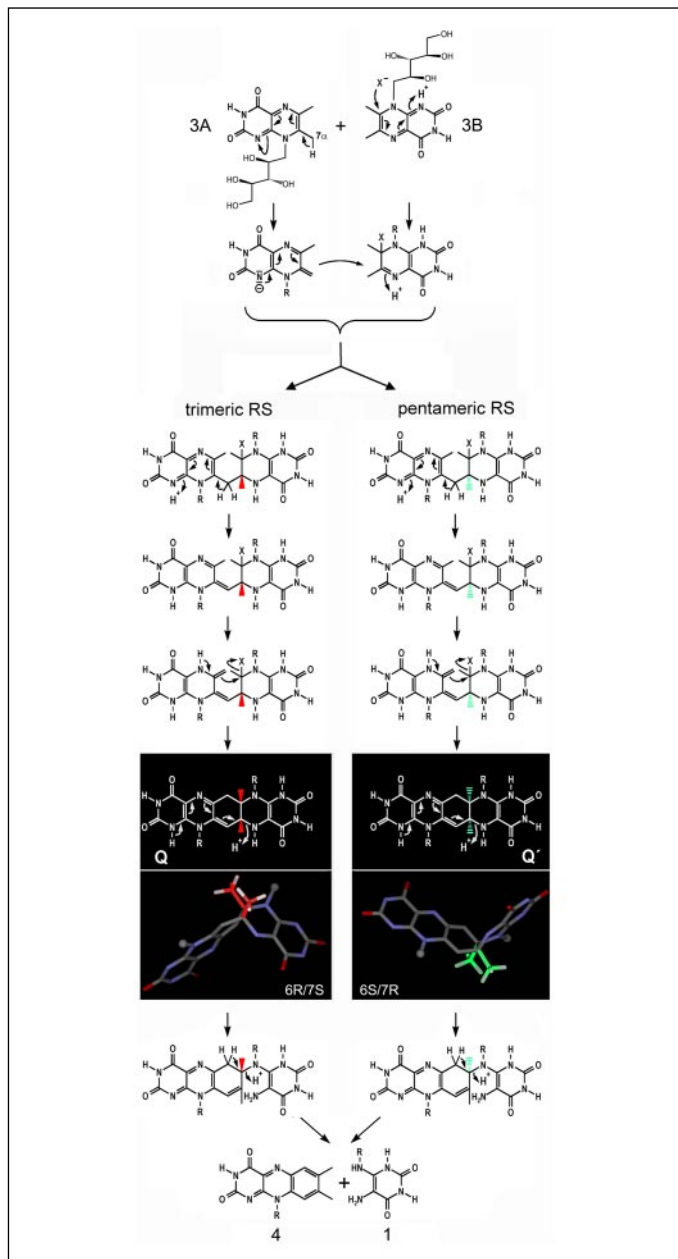


**FIGURE 7. Stereochemistry of 6,7-dimethyl-8-ribityllumazine conversion into riboflavin catalyzed by trimeric eubacterial and pentameric archaeal riboflavin synthase.** Binding of the substrates in anti-parallel orientation occurs at two sites, one leading to acceptance of a 4-carbon unit (**3A**, acceptor site) and the other to its donation (**3B**, donor site); **Q** and **Q'**, proposed pentacyclic reaction intermediates. *R*, ribityl (16, 39, 40). Reproduced with permission from Fischer *et al.* (4).

of the pentacyclic chromophore is lost in the final steps of the trajectory, and the stereochemical course of the reaction does not influence the stereochemistry of the products (which is exclusively determined by the chiral polyol side chains).

The fragmentation of the pentacyclic intermediates affording the products riboflavin and 5-amino-6-ribitylamino-2,4(1*H*,3*H*)-pyrimidine-dione (**1**) is believed to proceed via two consecutive and highly plausible elimination steps (Fig. 7) (40). On the other hand, the trajectory conducive to dimerization is far from clear. Early work by Plaut, Wood, Pfeiderer, and their respective groups had established that the position 7 methyl group of DMRL is acidic with a  $pK_a$  around 9 (41). This unusually high CH acidity has been attributed to the resonance stabilization of the lumazine anion (13, 42–44). The authors quoted above have proposed several variations on a common theme for the transformation of DMRL into riboflavin (11, 39, 40, 45, 46). Based on the x-ray structures reported in this work and in the paper by Gerhardt *et al.* (20) the hypothetical mechanism involving tricyclic adduct forms of DMRL can now be ruled out (20, 46).

Following the discovery of the pentacyclic intermediate, the consensus mechanism arising from the early work of the Wood and Plaut groups could be easily modified to incorporate the experimentally observed intermediate. Nevertheless, the revised mechanism (40) remains a matter of speculation, and the three-dimensional structures that are now available fail to resolve that dilemma. Thus, further study will be required on this highly unusual reaction that is conducive to the formation of one of the most widely used redox cofactor classes.

The riboflavin synthases of Archaea have no detectable sequence similarity with those of eubacteria, yeasts and plants. However, their sequences and structures closely resemble those of 6,7-dimethyl-8-ribityllumazine synthases. Completely sequenced archaeal genomes typically comprise sets of two similar genes, which specify a riboflavin synthase and a lumazine synthase. Sequence arguments also showed that the divergence between the paralogous lumazine synthases and riboflavin synthases occurred early in evolution (21).

The five topologically equivalent active sites of pentameric lumazine synthases are located at the interfaces between adjacent monomers of the pentamer. Two substrates, 3,4-dihydroxy-2-butanone 4-phosphate (**2**) and 5-amino-6-(D-ribitylamino)-2,4(1*H*,3*H*)-pyrimidinedione (**1**), have to be bound in the active site (38, 47–52). Recent studies with the lumazine synthase from *B. subtilis* suggested that the rate enhancement by the lumazine synthase is predominantly achieved by establishing a favorable topological relation of the two substrates.

The cavity harboring the active site of the closely related pentameric riboflavin synthase of *M. jannaschii* is similar to that of lumazine synthases, but the enzyme has no detectable lumazine synthase activity.

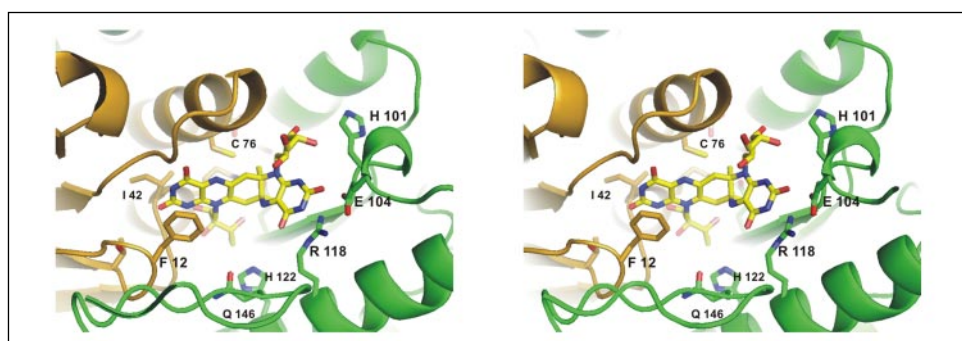


**FIGURE 8. Pentacyclic adduct of two DMRL molecules, with 6S/7R configuration modeled into the proposed active site of *M. jannaschii* riboflavin synthase (39).**

## Structure of Riboflavin Synthase of *M. jannaschii*

The binding mode of lumazine molecule **A** in pentameric riboflavin synthase closely resembles the pyrimidinedione binding site of lumazine synthases. On the other hand, the other part of the active site cavity forming the binding site for lumazine molecule **B** is structurally rather different compared with lumazine synthases (Fig. 3). Hence, it is not surprising that the activity of the ancestor is lost in pentameric riboflavin synthases.

**Acknowledgment—**We thank Dr. Peter Goettig for his expert technical assistance.

### REFERENCES

1. Fischer, M., and Bacher, A. (2005) *Nat. Prod. Rep.* **22**, 324–350
2. Bacher, A., Eberhardt, S., Fischer, M., Kis, K., and Richter, G. (2000) *Annu. Rev. Nutr.* **20**, 153–167
3. Bacher, A., Eberhardt, S., Eisenreich, W., Fischer, M., Herz, S., Illarionov, B., Kis, K., and Richter, G. (2001) *Vitam. Horm.* **61**, 1–49
4. Fischer, M., Römisich, W., Illarionov, B., Eisenreich, W., and Bacher, A. (2005) *Biochem. Soc. Trans.* **33**, 780–784
5. Echt, S., Bauer, S., Steinbacher, S., Huber, R., Bacher, A., and Fischer, M. (2004) *J. Mol. Biol.* **341**, 1085–1096
6. Chen, J., Illarionov, B., Bacher, A., Fischer, M., Haase, I., Georg, G., Ye, Q. Z., Ma, Z., and Cushman, M. (2005) *Anal. Biochem.* **338**, 124–130
7. Morgunova, E., Meining, W., Illarionov, B., Haase, I., Bacher, A., Cushman, M., Fischer, M., and Ladenstein, R. (2005) *Biochemistry* **44**, 2746–2758
8. Volk, R., and Bacher, A. (1988) *J. Am. Chem. Soc.* **110**, 3651–3653
9. Kis, K., and Bacher, A. (1995) *J. Biol. Chem.* **270**, 16788–16795
10. Wacker, H., Harvey, R. A., Winestock, C. H., and Plaut, G. W. (1964) *J. Biol. Chem.* **239**, 3493–3497
11. Paterson, T., and Wood, H. C. S. (1969) *J. Chem. Soc. Commun.* 290–291
12. Sedlmaier, H., Müller, F., Keller, P. J., and Bacher, A. (1987) *Z. Naturforsch. (C)* **42**, 425–429
13. Beach, R. L., and Plaut, G. W. E. (1970) *Biochemistry* **9**, 760–770
14. Plaut, G. W. E. (1963) *J. Biol. Chem.* **238**, 2225–2243
15. Rowan, T., and Wood, H. C. S. (1963) *Proc. Chem. Soc.* 21–22
16. Beach, R. L., and Plaut, G. W. E. (1970) *J. Am. Chem. Soc.* **92**, 2913–2916
17. Kis, K., Kugelbrey, K., and Bacher, A. (2001) *J. Org. Chem.* **66**, 2555–2559
18. Bacher, A., and Mailänder, B. (1978) *J. Bacteriol.* **134**, 476–482
19. Bacher, A., Baur, R., Eggers, U., Harders, H. D., Otto, M. K., and Schneppele, H. (1980) *J. Biol. Chem.* **255**, 632–637
20. Gerhardt, S., Schott, A. K., Kairies, N., Cushman, M., Illarionov, B., Eisenreich, W., Bacher, A., Huber, R., Steinbacher, S., and Fischer, M. (2002) *Structure (Camb.)* **10**, 1371–1381
21. Fischer, M., Schott, A. K., Römisich, W., Ramsperger, A., Augustin, M., Fidler, A., Bacher, A., Richter, G., Huber, R., and Eisenreich, W. (2004) *J. Mol. Biol.* **343**, 267–278
22. Leslie, A. G. W. (1999) *Acta Crystallogr. Sect. D Biol. Crystallogr.* **55**, 1696–1702
23. Bailey, S. (1994) *Acta Crystallogr. Sect. D Biol. Crystallogr.* **50**, 760–763
24. Otwinowski, Z., and Minor, W. (1997) *Macromol. Crystallogr.* **276**, 307–326
25. Weeks, C. M., and Miller, R. (1999) *J. Appl. Crystallogr.* **32**, 120–124
26. Bricogne, G., Vonrhein, C., Flensburg, C., Schiltz, M., and Paciorek, W. (2003) *Acta Crystallogr. Sect. D Biol. Crystallogr.* **59**, 2023–2030
27. Terwilliger, T. C. (2001) *Acta Crystallogr. Sect. D Biol. Crystallogr.* **57**, 1763–1775
28. Turk, D. (1992) *Development of a Program for the Manipulation of Molecular Graphics and Electron Densities and Their Usage for Protein Structure Analysis*. Ph.D. thesis, Technische Universität München, Garching, Germany
29. Brunger, A. T., Adams, P. D., Clore, G. M., DeLano, W. L., Gros, P., Grosse-Kunstleve, R. W., Jiang, J. S., Kuszewski, J., Nilges, M., Pannu, N. S., Read, R. J., Rice, L. M., Simonson, T., and Warren, G. L. (1998) *Acta Crystallogr. Sect. D Biol. Crystallogr.* **54**, 905–921
30. Engh, R. A., and Huber, R. (1991) *Acta Crystallogr. Sect. A* **47**, 392–400
31. Murshudov, G. N., Vagin, A. A., and Dodson, E. J. (1997) *Acta Crystallogr. Sect. D Biol. Crystallogr.* **53**, 240–255
32. Tripos, I. (1998) *Sybyl Molecular Modeling System* 6.7, St. Louis, MO
33. Laskowski, R. A. (2001) *Nucleic Acids Res.* **29**, 221–222
34. Lu, G. G. (2000) *J. Appl. Crystallogr.* **33**, 176–183
35. Kraulis, P. J. (1991) *J. Appl. Crystallogr.* **24**, 946–950
36. DeLano, W. L. (2002) *PYMOL*, DeLano Scientific, San Carlos, CA
37. Holm, L., and Sander, C. (1993) *J. Mol. Biol.* **233**, 123–138
38. Gerhardt, S., Haase, I., Steinbacher, S., Kaiser, J. T., Cushman, M., Bacher, A., Huber, R., and Fischer, M. (2002) *J. Mol. Biol.* **318**, 1317–1329
39. Illarionov, B., Eisenreich, W., Schramek, N., Bacher, A., and Fischer, M. (2005) *J. Biol. Chem.* **280**, 28541–28546
40. Illarionov, B., Eisenreich, W., and Bacher, A. (2001) *Proc. Natl. Acad. Sci. U. S. A.* **98**, 7224–7229
41. Pfeiderer, W., and Hutzenlaub, W. (1973) *Chem. Ber.* **106**, 3149–3174
42. Pfeiderer, W., Mengel, R., and Hemmerich, P. (1971) *Chem. Ber.* **104**, 2273–2292
43. Bown, D. H., Keller, P. J., Floss, H. G., Sedlmaier, H., and Bacher, A. (1986) *J. Org. Chem.* **51**, 2461–2467
44. Beach, R. L., and Plaut, G. W. E. (1971) *J. Org. Chem.* **36**, 3937–3943
45. Truffault, V. (2002) *Solution State NMR Investigations on the Structure and Function of Proteins: Application to Riboflavin Synthase*. Ph.D. thesis, Technische Universität München, Garching, Germany
46. Plaut, G. W. E., and Beach, R. L. (1976) in *Flavins and Flavoproteins, Proceedings of the 5th International Symposium* (Singer, T. P., ed) pp. 737–746, Elsevier Scientific Publishing Co., Amsterdam
47. Koch, M., Breithaupt, C., Gerhardt, S., Haase, I., Weber, S., Cushman, M., Huber, R., Bacher, A., and Fischer, M. (2004) *Eur. J. Biochem.* **271**, 3208–3214
48. Meining, W., Mörtl, S., Fischer, M., Cushman, M., Bacher, A., and Ladenstein, R. (2000) *J. Mol. Biol.* **299**, 181–197
49. Ladenstein, R., Schneider, M., Huber, R., Bartunik, H. D., Wilson, K., Schott, K., and Bacher, A. (1988) *J. Mol. Biol.* **203**, 1045–1070
50. Ladenstein, R., Ritsert, K., Huber, R., Richter, G., and Bacher, A. (1994) *Eur. J. Biochem.* **223**, 1007–1017
51. Persson, K., Schneider, G., Douglas, B. J., Viitanen, P. V., and Sandalova, T. (1999) *Protein Sci.* **8**, 2355–2365
52. Ritsert, K., Huber, R., Turk, D., Ladenstein, R., Schmidt-Bäse, K., and Bacher, A. (1995) *J. Mol. Biol.* **253**, 151–167
53. Thompson, J. D., Higgins, D. G., and Gibson, T. J. (1994) *Nucleic Acids Res.* **22**, 4673–4680